Carbohydrate Polymers **21** (1993) 249–259

Phase equilibria and gelation in gelatin/maltodextrin systems — Part II: polymer incompatibility in solution

Stefan Kasapis, Edwin R. Morris

Department of Food Research and Technology, Cranfield Institute of Technology, Silsoe College, Silsoe, Bedford MK45 4DT, UK

Ian T. Norton & Michael J. Gidley

Unilever Research, Colworth Laboratory, Sharnbrook, Bedford MK44 1LQ, UK

(Received 21 January 1993; accepted 26 February 1993)

The effect of thermodynamic incompatibility in mixed solutions of gelatin and Paselli maltodextrins SA-6 and SA-2 has been studied at a temperature (45°C) where the individual polymers are stable as disordered coils. Concentrated mixtures of SA-6 and gelatin showed classic phase separation into two co-existing liquid layers, with compositions lying along a well-defined binodal. On decreasing SA-6 concentration below the binodal, however, a substantial proportion (up to 60%) of the maltodextrin was precipitated, with normal single-phase solutions occurring only at much lower concentrations of both polymers. SA-2 showed a more extreme version of the same behaviour, with precipitation of up to 100% of the maltodextrin and no evidence of co-existing liquid phases at any accessible concentrations. In both cases, the amount of maltodextrin precipitated was proportional to the square of its initial concentration and to the first power of gelatin concentration, indicating that gelatin drives self-association and aggregation of maltodextrin when both polymers are present in a single liquid phase. ^{1}H NMR showed the precipitated maltodextrin to be higher in molecular weight and in degree of branching than the material remaining in solution, and particle-size analysis indicated that the volume of the individual maltodextrin particles increased linearly with the total mass precipitated.

1 INTRODUCTION

When concentrated solutions of two different polymers are mixed together, the mixture will often immediately become cloudy and, over a period of time, separate into two clear layers, with each containing most of one polymer and little of the other. This phenomenon of 'phase separation' is well understood (Flory & Rehner, 1943; Morawetz, 1965; Koningsveld, 1968; Albertsson, 1970), and contrasts with the behaviour of small molecules, which normally remain intimately mixed. In both cases the difference in free energy between the single-phase and biphasic states depends, as in any chemical system, on the entropy–enthalpy balance. For solutions of small molecules, entropy of mixing within a single phase usually outweighs any enthalpic interactions between the dissolved species, unless these interactions are very strong (e.g. precipitation of salts in which both ions have a high charge). In polymer solutions, where there are, of course, far fewer independently-moving species, the entropic advantage of mixing is grossly reduced and the enthalpy of interaction becomes dominant. If the interaction is favourable (e.g. polyanion–polycation) the two polymers may associate into a single gel-like phase or solid precipitate (Tolstoguzov & Wajnermann, 1975). Such behaviour is widely used in encapsulation technology. The more usual situation, however, is for interactions between segments of two different polymers to be less favourable than those between like chains of each type. It is this 'thermodynamic incompatibility' that gives rise to phase separation.

Carbohydrate Polymers 0144-8617/93/$06.00

The initial turbidity immediately after mixing is caused by one phase being dispersed as fine droplets within the other. Resolution into co-existing layers depends on differences in the density of the two phases, and can be accelerated by centrifugation. If the concentration of one polymer is held constant, phase separation will occur only when the concentration of the other exceeds a minimum critical value, which decreases as the concentration of the first component is raised. Combinations of polymer concentration corresponding to the onset of phase separation (with consequent cloudiness on mixing) define a 'cloud point curve' (or 'binodal') between monophasic and biphasic systems. In practice, such cloud point curves are normally obtained by measurement of the composition of the co-existing layers after phase separation (since each layer is then effectively a solution of one polymer 'saturated' with the other to the maximum concentration possible within the same phase).

At concentrations below the binodal, where the polymers remain mixed in a single phase, the thermodynamic incompatibility may still produce major changes in behaviour, by discouraging interpenetration of unlike chains, so that the two polymers are, in effect, competing for the same space. In particular, if one component can undergo a disorder–order transition, the presence of the other may drive conversion to the more compact ordered form. The effect of mutual exclusion on the rate of network formation in gelatin–maltodextrin mixed gel systems is demonstrated in the following paper (Kasapis *et al.*, 1993*b*; Part III of this series). The present paper explores the consequences of polymer incompatibility in solution.

2 EXPERIMENTAL PROCEDURE

The materials used were identical to those described in the preceding paper (Kasapis *et al.*, 1993*a*): second-extract limed-ossein gelatin (LO-2) and Paselli maltodextrins SA-6 and SA-2. Phase separation in mixed protein–polysaccharide solutions normally occurs at a total polymer concentration of about 4% (Tolstoguzov, 1986), although the exact value can, of course, vary significantly from system to system. Because of the low molecular weight of maltodextrins, solutions can be prepared to unusually high concentrations, substantially above the minimum values anticipated for phase separation with gelatin. In the present work, the concentrations of maltodextrin used were in the range 5–25% (w/w).

The experiments were carried out at 45°C, chosen to be well above the onset of conformational ordering for the gelatin sample used (Busnel *et al.*, 1988) but still conveniently low for laboratory manipulation. At this temperature, the maltodextrin samples were also expected to remain as disordered coils in solution over the timescale of the experiments. In the preceding paper (Kasapis *et al.*, 1993*a*) simple equations were developed to relate the gel time for SA-6 and SA-2 to polymer concentration and temperature. For the maltodextrin concentrations used, the times calculated in this way for the onset of gelation in SA-2 at 45°C range from about 3 h (at 25% (w/w)) to about 6 months (at 5% (w/w)), and the corresponding range for SA-6 is from about 5 days to over 2000 years! By comparison, the entire experimental procedure (detailed below) took less than 1 h.

Stock solutions of gelatin and maltodextrin were prepared as described previously (Kasapis *et al.*, 1993*a*) and held at 50°C. Experimental samples were made by mixing appropriate weights of the individual solutions. After weighing, it was confirmed that the temperature had not fallen below 45°C.

At low concentrations the mixed solutions remained clear, but at higher concentrations they showed the immediate cloudiness indicative of phase separation. To accelerate resolution of the initial fine emulsion into two discrete liquid layers, the samples were placed immediately in a pre-heated rotor and centrifuged at 45°C for 30 min at 1150 g (3000 rpm on a Sorval Superspeed centrifuge). The resulting liquid layers were then separated by careful use of a Pasteur pipette, weighed, and analysed for maltodextrin and gelatin concentration by optical rotation. The principle of the analysis is outlined in the following section. Measurements were made on a Perkin-Elmer 241 polarimeter using a jacketed 1-cm cell, with temperature maintained at 45 ± 0·5°C by a Haake circulating water bath and monitored by a thermocouple in the neck of the cell.

3 ANALYSIS OF PHASE COMPOSITION BY OPTICAL ROTATION

The analysis is based on the simple principle that the measured optical rotation of a mixed solution is the linear sum of the optical rotation contributions from the individual components, which will in turn be directly proportional to their concentration:

$$\alpha(\lambda) = c_1\,\alpha_1(\lambda) + c_2\,\alpha_2(\lambda) \qquad (1)$$

where c_1 and c_2 are the concentrations of the two polymers, $\alpha_1(\lambda)$ and $\alpha_2(\lambda)$ denote their optical rotation per unit concentration at wavelength λ, and $\alpha(\lambda)$ is the overall, observed optical rotation of the mixture at the same wavelength. Thus by measurement at two different wavelengths, the values of c_1 and c_2 can be derived by solution of the two resulting simultaneous equations. In practice, optical rotation values were measured at four wavelengths available as mercury emission lines on the polarimeter (365, 436, 546 and 578 nm), and the best fitting values of c_1 and c_2 were obtained by a simple least-squares computer analysis.

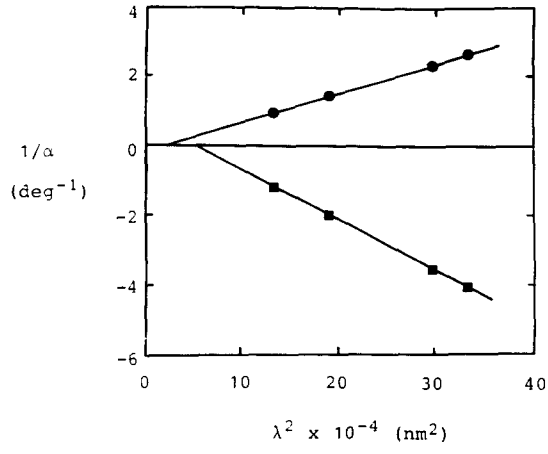

Fig. 1. Drude plots for 2% (w/w) solutions of LO-2 (■) and SA-6 (●) at 45°C, measured at wavelengths of 365, 436, 546 and 578 nm in a 1-cm cell.

The values of $\alpha_1(\lambda)$ and $\alpha_2(\lambda)$ used in the program were derived from calibration plots of α versus c for the individual polymers (with SA-6 and SA-2 giving essentially identical optical rotation). The reliability of the calibration values at each concentration of both polymers was checked by constructing Drude plots (Djerassi, 1960) of $1/\alpha$ versus λ^2. The standard of linearity achieved is illustrated in Fig. 1. Linear Drude plots were also obtained for the mixed solutions present in the upper and lower layers after phase separation.

As a point of practical detail, all concentrations in this work are expressed on a weight basis (since weight can, of course, be measured with far greater accuracy than volume). Optical rotation, however, is directly proportional to concentration per unit volume, so that the calibration plots of α versus c (% (w/w)) showed significant curvature. The difficulty was eliminated by including in the computer program a simple empirical function to convert concentrations to % (w/v) before applying eqn (1), and to reconvert to % (w/w) for output of the fitted values.

The reliability of the method was established by analysis of a range of mixtures of known composition, yielding results in excellent agreement (to within ± 1%) with the expected values. Since optical rotation at four wavelengths can be measured in about 1 min, this procedure represents a considerable saving in time and effort, and a considerable gain in accuracy, over traditional methods such as the phenol-sulphuric acid assay for carbohydrates and optical density at 280 nm for proteins. It should be noted, however, that the analysis can be applied only if the fractional change in optical rotation on going from one wavelength to another is different for the two materials under investigation; otherwise the concentration/optical rotation relationship indicated in eqn (1) will become degenerate. The difference in the wavelength-dependence of optical rotation for gelatin and maltodextrins is shown by the Drude plots in Fig. 1, with $1/\alpha$ extrapolating to zero at different values of λ^2.

4 PHASE SEPARATION AT HIGH CONCENTRATION

Figure 2 shows the phase diagram obtained for LO-2 and SA-6 at pH 7 and temperature 45°C. At combinations above about 2% LO-2 and about 20% SA-6 the thermodynamic incompatibility of the two polymers induces classic phase separation, giving two co-existing liquid phases, one enriched in LO-2 and depleted in SA-6 (upper layer) and the other SA-6 enriched and LO-2 depleted (lower layer). Table 1 lists the initial composition of the mixed solutions and the final composition and weight of the individual phases.

The points defining the composition of each phase

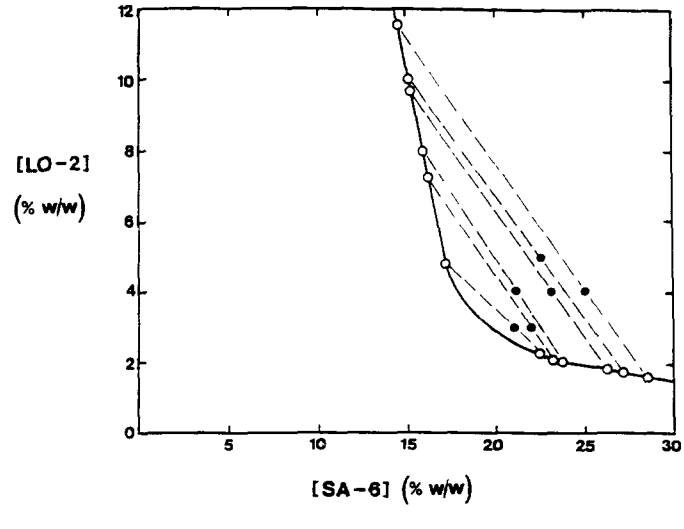

Fig. 2. Phase-separation in concentrated mixed solutions of SA-6 and LO-2 at 45°C. Compositions of co-existing liquid layers (○) lying along the binodal (——) are joined by tie lines (– – –) passing through the composition of the original mixed solution (●).

Table 1. Phase-separation in mixed solutions of gelatin (LO-2) and maltodextrin (SA-6) at 45°C. The composition of the gelatin-rich (upper) and maltodextrin-rich (lower) layers were used to construct the phase diagram shown in Fig. 2

LO-2 concentration (% w/w)			SA-6 concentration (% w/w)			Weight of phases (g)		
Total	Upper	Lower	Total	Upper	Lower	Total	Upper	Lower
3·00	4·77	2·37	21·0	17·1	22·4	9·65	2·53	7·12
3·00	7·31	1·99	22·0	16·2	23·4	9·99	1·89	8·10
4·00	8·00	1·95	21·0	16·0	23·6	10·01	3·40	6·61
4·00	9·72	1·84	21·0	15·1	26·3	10·01	2·77	7·24
4·00	11·55	1·50	25·0	14·4	28·6	10·02	2·43	7·59
5·00	10·01	1·85	22·5	15·2	27·1	9·08	3·50	5·58

(Table 1) lie along the binodal, or 'cloud point curve' (bold line in Fig. 2) and the tie line joining them passes through the point corresponding to the initial composition of the mixture (i.e. the overall concentrations of LO-2 and SA-6). As the concentration decreases, the family of tie lines degenerates to a single critical point (at about 3% LO-2 and 20% SA-6), defined (Zhuravskaya *et al.*, 1986) by the intercept of the binodal with the curve linking the mid-points of each tie line (Fig. 3). The phase diagram is highly asymmetric, as reflected in the difference in the axis scales, so that the final concentrations of SA-6 in the lower phase are very much higher than the concentrations of LO-2 in the upper phase. This is an expected consequence of the larger volume occupied by the gelatin chains, due to their expanded coil dimensions and high molecular weight in comparison with SA-6.

5 PRECIPITATION AT LOWER CONCENTRATIONS

The results presented so far, for high concentrations of SA-6 and LO-2, are typical of those obtained for many other mixed biopolymer systems (see for example Tolstoguzov, 1986, 1988, 1991). At somewhat lower concentrations, however, the system displayed totally unexpected, and extremely unusual, behaviour. When the concentration of SA-6 was reduced to below the binodal, the mixed solution did not remain in a single phase as expected, but instead produced an insoluble, densely-packed, clay-like precipitate, whose volume in extreme cases was as much as a third of the total.

The combinations of SA-6 and LO-2 concentrations at which this unusual behaviour was observed are shown in Fig. 3. All mixtures whose initial composition lay in the area of the phase diagram bounded by the binodal and the (less well-defined) line at lower concentration gave precipitates after centrifugation. The expected, normal, single-phase behaviour was observed only between the second line and the concentration axes. To verify that centrifugation was simply compacting existing particles rather than inducing their formation, a few representative samples were allowed to sediment under gravity over a period of about a month in an incubator at 45°C. The amount and composition of the precipitates were closely similar to those observed after centrifugation.

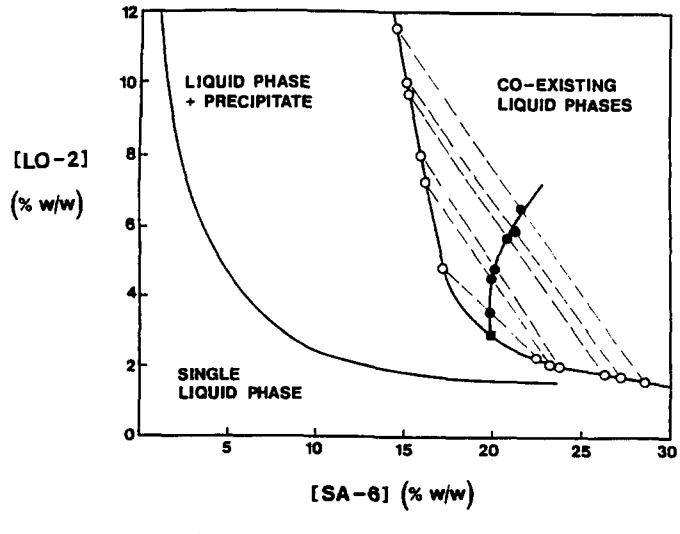

Fig. 3. Phase behaviour of SA-6 and LO-2 in mixed solutions at 45°C. The mid-points (●) of the tie lines linking co-existing liquid phases (○) are extrapolated to the single critical point (■) on the binodal. Regions of composition giving single-phase behaviour, or precipitation of maltodextrin from solution, are also indicated.

Similar experiments using LO-2 in combination with SA-2 instead of SA-6 showed a more extreme version of the same behaviour, the volume of the packed precipitate obtained after centrifugation being in some cases more than 80% of the total sample volume. 'Classic' phase separation into co-existing liquid layers did not occur for this system at any experimentally-accessible combinations of LO-2 and SA-2 concentration. Either precipitation was observed or, at lower concentrations, the mixture remained as a single-phase solution (behaviour analogous to the second line in the phase diagram for SA-6/LO-2 in Fig. 3).

To determine their composition, the precipitates were dispersed in the amount of water required to give 10-fold dilution, re-dissolved at high temperature (90°C) and analysed by optical rotation at 45°C (with the values obtained being multiplied by 10 to give the concentrations in the original precipitate). The absolute amounts precipitated were then calculated from the overall weight of the precipitate (Table 2).

Most of the precipitates were composed predominantly of maltodextrin (and water). The measured content of gelatin was comparable to that of maltodextrin only in systems where very little precipitate was formed (making separation from the solution phase particularly difficult). Otherwise, the gelatin content was normally less than 10% of the total polymer content, was in some cases undetectable, and showed no systematic correlation with overall composition (in contrast to the direct correlation described later for maltodextrin), strongly suggesting that it was due solely to slight cross-contamination in separation of the precipitate from the (gelatin-rich) solution.

6 NMR ANALYSIS OF DISSOLVED AND PRECIPITATED MALTODEXTRIN

The composition of maltodextrin in precipitates, supernatants and co-existing liquid phases was characterised by ^{1}H NMR (Gidley, 1985). Figure 4 shows the anomeric proton region from an illustrative spectrum obtained for SA-6 at 90°C (recorded at 200 MHz on a Bruker AM200, using a 90° observation pulse and a delay of 15 s between consecutive pulses to ensure complete relaxation). It comprises four doublets assigned to H(1) of reducing end-groups in the α and β configurations (at 5·27 and 4·68 ppm, respectively), the anomeric protons at 1,6 branch points (5·00 ppm) and the main signal at 5·40 ppm from the anomeric protons of 1,4 linkages. Integration of these resolvable resonances gives the degree of branching (from the ratio of the signals arising from 1,6 and 1,4 linkages) and the 'dextrose equivalent' (from the combined intensity of the resonances from α and β end-groups relative to the total anomeric signal). The DE values obtained for the batches of SA-6 and

Table 2. Precipitation of maltodextrin starch hydrolysis products (SHP) SA-6 and SA-2 from mixed solutions with gelatin (LO-2) at 45°C

	Total weights (g/100 g)				Concentrations (% w/w)				Percent precipitated	
	SHP	LO-2	Solution	Precipitate	Solution		Precipitate		SHP	LO-2
					SHP	LO-2	SHP	LO-2		
SA-6	5·0	7·0	92·8	7·2	4·9	7·2	9·5	4·8	13·7	5·0
	5·0	9·0	90·3	9·7	4·9	9·1	9·1	6·6	17·6	7·1
	7·0	4·0	94·4	5·6	6·6	4·4	15·9	2·5	12·7	3·4
	7·0	6·0	90·4	9·6	6·3	6·5	13·8	4·4	18·9	7·0
	10·0	3·0	92·5	7·5	9·7	3·3	14·5	0·0	10·9	0·0
	10·0	6·0	86·5	12·5	8·8	6·4	17·1	4·8	21·3	10·0
	10·0	7·0	81·9	18·1	9·6	7·1	13·8	5·3	25·0	13·7
	10·0	10·0	81·8	18·8	9·2	11·3	19·0	1·8	35·8	3·4
	10·0	12·0	80·8	19·2	7·9	14·2	23·7	1·5	45·4	2·4
	12·0	5·0	82·9	17·1	11·4	5·4	17·4	2·2	24·8	7·6
	12·0	9·0	78·9	21·1	8·9	11·4	25·3	1·2	44·6	2·8
	15·0	7·0	71·4	28·6	12·8	8·7	22·6	1·8	43·2	7·2
	15·0	10·0	66·4	33·6	10·0	14·0	27·7	1·1	61·9	3·8
SA-2	5·0	4·0	95·2	4·8	4·5	4·2	15·1	0·8	14·5	0·9
	5·0	7·0	89·8	10·2	4·0	7·8	14·0	0·0	28·3	0·0
	7·0	7·0	77·5	22·5	5·6	8·7	11·7	1·1	37·5	3·7
	10·0	10·0	64·4	35·6	2·1	14·8	24·3	1·3	86·6	4·7
	12·0	7·0	56·9	43·1	5·6	12·3	20·4	0·0	73·1	0·0
	15·0	4·0	61·9	38·1	11·7	6·0	20·4	0·7	52·0	6·8
	17·0	6·0	40·3	59·7	6·3	14·7	24·2	0·2	85·1	1·7
	20·0	6·0	28·2	71·8	0·0	17·5	28·0	1·5	100·0	17·5
	23·0	4·0	17·6	82·4	22·9	22·8	23·0	0·0	82·5	0·0
	24·0	4·0	24·8	75·2	11·7	16·2	28·0	0·0	87·8	0·0

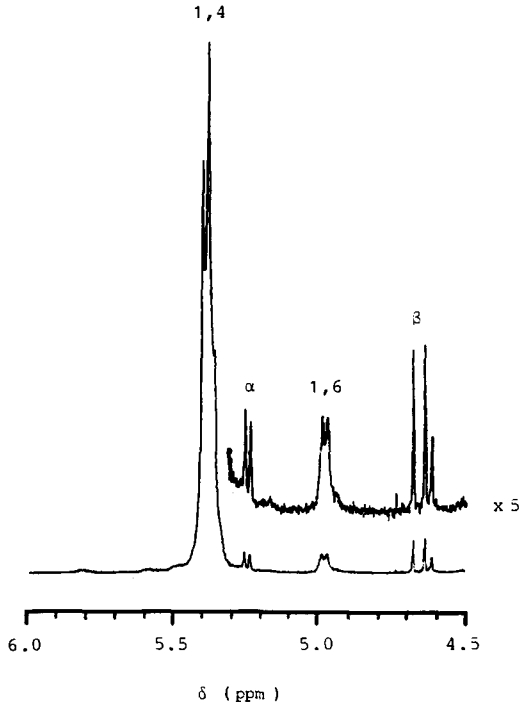

Fi. 4. High-resolution ^1H NMR (200 MHz) of SA-6 at 90°C in D_2O. The doublets arising from anomeric protons of 1,4 linkages, 1,6 branch points and reducing end-groups in the α and β configurations are indicated.

SA-2 used (Table 3) were, respectively, 4·3 and 2·9 (appreciably different from the nominal values of 6 and 2).

In mixed solutions with gelatin, the signal from end-groups in the β configuration was obscured, but there was no interference with the resonances from α-anomers, allowing the content of reducing ends to be determined from the anomeric equilibrium value obtained for maltodextrin alone ($\alpha/\beta = 1{\cdot}095$). Three mixed systems of LO-2 and SA-6 were examined in this way: a combination giving only a very small amount of precipitate (7% SA-6 + 4% LO-2), one giving extensive precipitation (15·3% SA-6 + 10% LO-2), and one giving two co-existing liquid layers (22·5% SA-6 + 5% LO-2). These correspond to points just above the second line in Fig. 3, just below the binodal, and well above the binodal, respectively. In each case the composition of maltodextrin in the two phases (precipitate and supernatant or upper and lower layers) was characterised. A similar study was carried out for two combinations of LO-2 and SA-2, both giving substantial precipitation (5% LO-2 + 22% SA-2 and 8% LO-2 + 18% SA-2). The results are listed in Table 3.

There is an obvious trend to larger molecules (lower DE) with a higher degree of branching in the maltodextrin-rich phases (precipitates or lower layer), with a corresponding increase in the proportion of smaller, more linear species remaining in the gelatin-rich solution phase. This trend is in qualititative agreement with the known thermodynamic origin of polymer incompatibility phenomena. Preferential exclusion of larger species is an expected consequence of the inverse relationship between entropy of mixing and molecular weight. Branched species would also be expected to show greater resistance to interpenetration than linear chains of the same molecular weight, because of their higher segment-density.

The indication that the precipitates consist predominantly of branched molecules, which must obviously have come from the amylopectin fraction of the original starch, is consistent with their ability to re-dissolve at about 80°C, behaviour which is similar to that of amylopectin rather than amylose (Whistler & Paschall, 1967; Ring *et al.*, 1987).

7 EXTENT OF PRECIPITATION

When maltodextrin concentration was held constant, the fraction precipitated (Table 2) was directly proportional to the concentration of gelatin present, as illu-

Table 3. NMR analysis of SA-6 and SA-2, alone and in mixed systems with LO-2

System	Fraction	Degree of branching (%)	DE
SA-6 alone		3·0	4·3
7·0% SA-6 + 4·0% LO-2	Supernatant	3·0	4·9
	Precipitate	3·5	4·0
15·3% SA-6 + 10·0% LO-2	Supernatant	2·1	4·7
	Precipitate	3·9	3·8
22·5% SA-6 + 5·0% LO-2	Upper layer	2·3	6·3
	Lower layer	3·2	4·0
SA-2 alone		3·7	2·9
18·0% SA-2 + 8·0% LO-2	Supernatant	2·5	5·3
	Precipitate	4·1	2·7
22·0% SA-2 + 5·0% LO-2	Supernatant	2·1	5·3
	Precipitate	4·2	2·5

strated in Fig. 5. The slopes of the individual lines obtained at different concentrations of maltodextrin were themselves directly proportional to maltodextrin concentration (Fig. 6), yielding the following simple relationships:

$$\text{SA-6:} \quad f = 0{\cdot}40\,[\text{SA-6}]\,[\text{LO-2}] \tag{2}$$

$$\text{SA-2:} \quad f = 0{\cdot}84\,[\text{SA-2}]\,[\text{LO-2}] \tag{3}$$

The numerical coefficients relate to polymer concentrations expressed as % (w/w), and f denotes the fraction of maltodextrin precipitated, also expressed as a percentage. Thus, for example, application of eqn (2) to a mixed solution with initial concentrations of 10% (w/w) SA-6 and 5% (w/w) LO-2 would yield a value of 20% for the proportion of SA-6 precipitated, while for SA-2 the same initial concentrations would give 42% precipitation. The standard of agreement between observed and fitted values is shown in Fig. 7.

It should be emphasised that these relationships apply only to systems whose initial composition falls above minimum critical combinations of maltodextrin and gelatin concentration (as defined by the second line in the phase diagram in Fig. 3). In particular, no precipitation was observed for either SA-6 or SA-2 at LO-2 concentrations below about 2% (w/w). In the case of SA-6, there is the additional qualification that the initial composition should lie below the binodal.

In the above equations, the amount of maltodextrin precipitated is expressed as a fraction (f) of the total amount present. Thus the absolute amount precipitated (M) is proportional to f times the initial concentration, and hence from eqns (2) and (3):

$$M = k\,[\text{maltodextrin}]^2\,[\text{gelatin}] \tag{4}$$

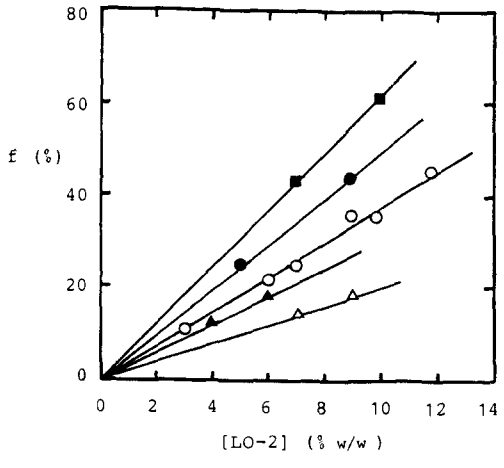

Fig. 5. Proportion (f) of maltodextrin precipitated from mixed solutions of SA-6 and LO-2 at 45°C. The dependence on gelatin concentration is shown for initial SA-6 concentrations (% w/w) of 5 (△), 7 (▲), 10 (○), 12 (●) and 15 (■).

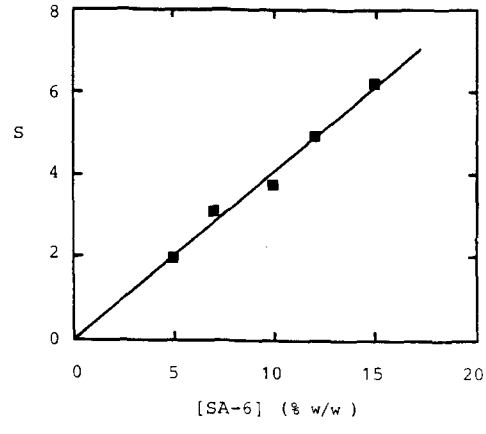

Fig. 6. Effect of the initial concentration of SA-6 on its extent of precipitation from mixed solutions with LO-2. S denotes the slope of the lines shown in Fig. 5 for the dependence on LO-2 concentration at fixed concentrations of SA-6.

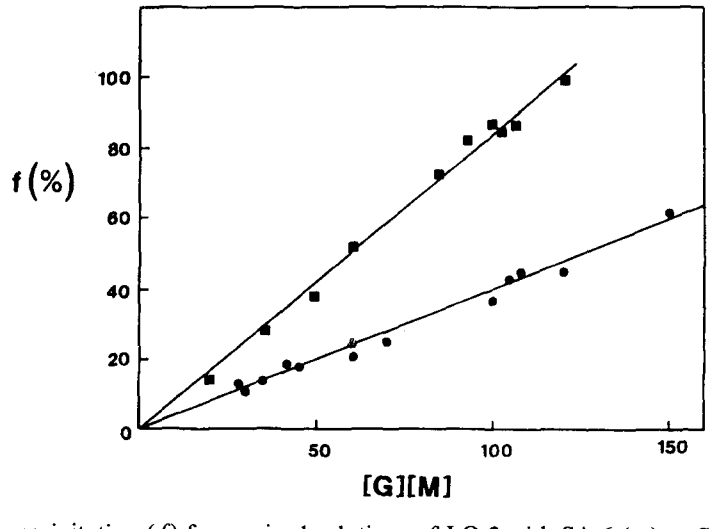

Fig. 7. Extent of maltodextrin precipitation (f) from mixed solutions of LO-2 with SA-6 (●) or SA-2 (■) at 45°C. [G] and [M] denote the initial concentrations (% w/w) of gelatin and maltodextrin, respectively. The lines are derived from eqns (2) and (3), and show the standard of agreement between observed and fitted values of f.

The form of this relationship indicates that precipitation follows a simple mass-action dependence on maltodextrin concentration, with gelatin driving the interaction by thermodynamic incompatability and exclusion when sufficient concentrations of the two polymers are present in a single phase.

The effect of the extent of precipitation on the size of the individual maltodextrin particles was studied by holding the SA-6 concentration constant (at 10% (w/w)) and varying the concentration of LO-2 between 4% and 12% (w/w), giving (eqn (2)) a three-fold increase in the amount of maltodextrin precipitated. Size measurements were made on a Malvern Master Sizer (a laser-diffraction instrument that can resolve particles with diameters in the range 0·1–2000 μm).

The mean particle diameter increased systematically from 52 μm for the precipitate formed in the presence of 4% (w/w) LO-2 (where 16% of the maltodextrin is precipitated) to 81 μm with 12% (w/w) LO-2 (48% precipitation of SA-6). As shown in Fig. 8, the average volume (calculated assuming spherical geometry) was approximately proportional to the total mass of maltodextrin precipitated, indicating that the number of particles formed remained roughly constant but that their volume (and hence their mass) increased linearly with increasing concentration of gelatin.

8 DISCUSSION AND CONCLUSIONS

It is well established that the central event in gelation or precipitation of starch-based polymers is association of 1,4-linked α-D-glucan chains into co-axial double helices, which can associate further by lateral aggregation (Gidley, 1989). The average helix length in amylose gels appears to be around 50–70 residues (Jane & Robyt, 1984; Clark *et al.*, 1989). Chains that are substantially longer than this can form helical junctions with more than one partner, leading to the development of a conventional gel network. Shorter chains, associating with only one helix-partner along their full length, form precipitates rather than gels.

The time/temperature course of these processes is strongly dependent on concentration and chainlength (Husemann *et al.*, 1963, 1964; Pfannemüller *et al.*, 1971; Gidley & Bulpin, 1989). In particular, the rate of aggregation of amylose, as monitored by light scattering in dilute solution (e.g. Pfannemüller *et al.*, 1971) or by development of turbidity at higher concentrations (Gidley & Bulpin, 1989) increases steeply with increasing chainlength, reaching a maximum at a degree of polymerisation (DP) of about 75–80. Monodisperse preparations of DP < 10 show no evidence of conformational ordering or association even under extreme forcing conditions of concentration, temperature and storage time (Gidley & Bulpin, 1987; Pfannemüller, 1987). Gelation of amylopectin appears to involve formation and subsequent crystallisation of helices just above this minimum threshold length (DP ≈ 15), and therefore occurs much more slowly than retrogradation or gelation of amylose (Gidley & Bulpin, 1987; Ring *et al.*, 1987).

The results of the present work indicate that conformational ordering (and consequent precipitation) of maltodextrins derived from potato starch, in which amylopectin predominates, can be grossly accelerated by the presence of gelatin in the same solution phase. Another obvious conclusion, however, is that when the

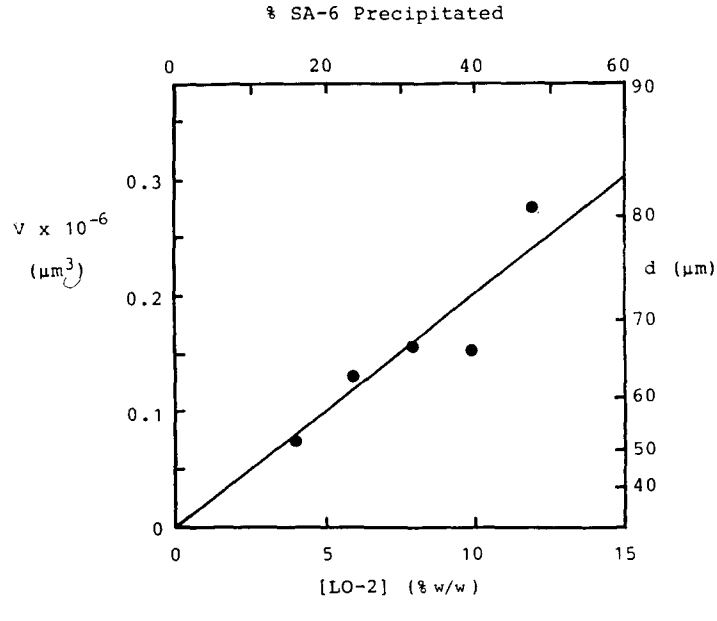

Fig. 8. Effect of LO-2 concentration on the average size of maltodextrin particles precipitated from mixed solution with 10% (w/w) SA-6 at 45°C. Mean diameters (d) from particle-size analysis (right-hand axis) were converted to mean volumes (V) by assuming spherical geometry. The fraction of maltodextrin precipitated (upper axis) was derived using eqn (2).

concentration of both polymers is sufficiently high, the system may resolve into two separate phases before any significant ordering has occurred.

The only unusual feature of the phase-separation behaviour observed for binary solutions of SA-6 and LO-2 is that it requires extremely high concentrations; the combined concentration of the two polymers at the critical point (Fig. 3) is about 23% (w/w), with values along the binodal lying in the range 22–30% (Table 1), in comparison with critical concentrations of around 4% for other protein–polysaccharide systems (Tolstoguzov, 1986). The difference, however, can reasonably be ascribed to the unusually low molecular weight of the maltodextrin component; the DE value of 4·3 obtained for SA-6 by NMR (Table 3) corresponds to a number-average degree of polymerisation of around 23 residues, in comparison with several thousand for intact polysaccharides.

The precipitation behaviour is less straightforward. Some aspects can be easily rationalised. The observation that SA-2, unlike SA-6, invariably responded to the presence of gelatin by precipitation rather than by resolution into a separate liquid phase is consistent with its much faster rate of self-association (Kasapis *et al.*, 1993*a*). The direct dependence of the amount of maltodextrin precipitated from single-phase solutions on the square of maltodextrin concentration and first power of gelatin concentration (eqn (4)) also seems consistent with the idea of gelatin promoting the association of pairs of disordered glucan chain-sequences into double helices. Detailed explanation of why this simple relationship should be obeyed is, however, far from trivial.

One tempting interpretation might be that the extent of precipitation is controlled by a solubility product for non-associated chains in the co-existing supernatant solution. This, however, can be dismissed by cursory inspection of the solution concentrations listed in Table 2. There is an obvious trend to higher concentrations of both maltodextrin and gelatin in the supernatant as their overall concentration throughout the entire system is increased. It would seem, therefore, that we must look for an explanation in the kinetics of structure formation, rather than in the equilibrium properties of the system after precipitation has occurred.

There are, however, two major problems in attempting to relate the observed precipitation behaviour to a simple kinetic scheme. The first is that we have found the extent of precipitation to correlate directly with the square of total maltodextrin concentration. A relationship of this type would be entirely reasonable for the initial rate of a two-coil to double helix transition. As in any chemical reaction, however, the rate should decrease as the starting material is used up, with a disproportionate reduction in average rate in systems where precipitation was extensive.

The second, more fundamental, problem is that the parameter observed experimentally was not the rate of precipitation but the total amount precipitated, which would relate directly to rate only if ordering was arrested after the same, fixed time in all cases. It seems unlikely that macroscopic separation (i.e. sedimentation of the precipitate) is responsible for terminating the reaction, first because the sediment is still in direct contact with the supernatant, and also because slow sedimentation under gravity gave the same final amount of precipitate as rapid sedimentation in a high-speed centrifuge. Results from previous studies of starch-based systems, however, suggest a possible explanation at the molecular level.

Although, as discussed above, conformational ordering in monodisperse amylose preparations occurs only at DP 10 and above, shorter oligomers, down to DP 6, have been found to co-crystallise with longer chains (Gidley & Bulpin, 1987). This behaviour cannot be explained simply by the oligomers forming double helices with the longer species, since the length (and hence the stability) of any such structures will, of course, be limited to the length of the shorter strand. Instead it must imply that long, stable helices can act as nuclei for formation of shorter helices, and then maintain the stability of the shorter structures by remaining co-operatively associated with them.

Analogous effects have been observed in studies of potato maltodextrins (Richter *et al.*, 1976; Schierbaum *et al.*, 1977) similar to those used in the present work. In an investigation by Schierbaum *et al.* (1986) it was found that the rate of gelation could be greatly increased by incorporating a small amount of intact amylose. 'Synergistic' interactions were also observed by Bulpin *et al.* (1984) between different fractions of the same maltodextrin, resolved by size-exclusion chromatography. Approximately half the sample was fully-excluded (minimum DP $\approx$ 60) and composed entirely of branched material from partial depolymerisation of amylopectin. The included fraction (approximate DP range 10–60) was predominantly linear, presumably originating from amylose and the outer chains of amylopectin. The correlation between molecular size and degree of branching is, of course, fully consistent with the NMR analyses from the present investigation (Table 3). Only the branched fraction was capable of forming gels, but these melted about 10°C lower than corresponding gels from the unfractionated material or from recombination of the isolated fractions. Both studies clearly indicate that linear chains can facilitate structuring of branched species.

It seems likely that the mechanism by which such facilitation occurs is similar to that proposed above for co-crystallisation of short oligomers with longer chains, and that it may be directly relevant to the precipitation phenomenon observed in the present work. Although it is evident that the linear chains in potato maltodextrins have a lower average molecular weight than the branched material, the determinant of helix stability is the length-

distribution of uninterrupted linear sequences rather than overall molecular size. The chromatographic analysis of Bulpin *et al.* (1984), and any reasonable interpretation of our own NMR results, would imply a significant population of linear chains appreciably longer than the helix structures observed (Ring *et al.*, 1987) for amylopectin (DP $\approx$ 15). We therefore propose the following model for precipitation of maltodextrin from mixed solutions.

On exposure to gelatin, at gelatin/maltodextrin concentrations below those required to cause immediate phase separation, the polymer exclusion effects discussed previously will drive conversion of maltodextrin from the disordered state to the more compact helical conformation. As in single-polymer solutions of amylose, long linear chains will order far more rapidly than the shorter sequences in branched species, to produce a small population of double helices. At this early stage of reaction there will be little depletion of the concentration of disordered sequences, so that the extent of ordering will be directly proportional to the square of the maltodextrin concentration. Also, since the process is driven by the presence of gelatin, a linear dependence on gelatin concentration does not seem unreasonable.

We then propose that, as discussed previously, these helices act as nuclei for very rapid ordering of shorter segments. Growth is likely to come mainly from the addition of branched species, first because of the preponderance of branched material present but also, more significantly, because the branching residues link together two linear strands which are immediately available as helix-partners, removing the necessity for a (statistically improbable) 'three-body collision' between the existing helix and two disordered chains moving independently. When species with more than one branching residue are added to the growing bundle, only the two chain-segments directly involved in helix-formation will be ordered; the other sequences will remain as a disordered 'fringe' surrounding the central core of aggregated helices, creating branched structures of very high molecular weight.

As discussed previously, large branched species are particularly effective in promoting phase-separation with other polymers. We therefore suggest that the next process in the cascade of events leading to precipitation is resolution of the system into two phases based, respectively, on gelatin and on the branched, nucleated aggregates proposed above. For obvious reasons of compatibility, unreacted branched material from the original population of maltodextrin chains is likely to partition with the aggregates, whereas linear species, because of their lower thermodynamic-incompatibility with gelatin, are likely to satisfy the entropic requirement for some maltodextrin to remain in the gelatin-rich phase.

At this stage, which we envisage being reached within a few seconds after initial mixing, formation of new aggregates will be essentially abolished, because the large branched species which constitute the bulk of the aggregated assemblies are now separated from the extended linear sequence required to trigger conformational ordering. Within the maltodextrin phase, however, the existing aggregates may continue to consolidate and grow until the ordered core becomes totally screened by the disordered fringe. Formation of a macroscopic precipitate would then occur by sedimentation of the final aggregated clusters.

In summary, the essential features of this (highly speculative) interpretation are:

(1) an initial rate-limiting process in which a small proportion of the linear chains undergo a coil–helix transition, following 'initial-slope' kinetics;
(2) rapid growth of large aggregates by the addition of branched material to the linear helices; and
(3) termination by phase-separation, removing the linear chains (which initiate ordering) from the branched species (which are needed to develop large aggregates).

Finally, the proposal of a 'synergistic' interaction between linear and branched chains provides an immediate explanation of why no precipitation occurred in the co-existing liquid layers formed on phase-separation of concentrated solutions of SA-6 and LO-2. As shown in Fig. 3, the concentration of gelatin in the maltodextrin-rich (lower) layers was reduced below the level required to induce precipitation of SA-6. In the associated upper layers, however, the gelatin concentrations were within the range observed (Table 2) to cause substantial precipitation, and the maltodextrin concentrations were higher than those in most of the precipitating systems.

The likely interpretation of this apparently puzzling behaviour is indicated by the NMR results shown in Table 3. In the phase-separating system analysed (22·5% SA-6 in combination with 5·0% LO-2), resolution of the maltodextrin into large, branched species in the lower layer and smaller, more-linear chains in the gelatin-rich phase was even more extreme than the differences in composition observed between precipitates and supernatants. Thus although the upper layer contains a high total concentration of maltodextrin, it is severely depleted in the large, branched molecules that appear to be essential for extensive association into large aggregates.

ACKNOWLEDGEMENTS

The authors thank Mr D. Caswell for recording the NMR spectra, Mr P.J. Hart for expert advice on particle-size measurement, and Dr A.H. Clark for many helpful discussions.

REFERENCES

Albertsson, P.-Å. (1970). *Adv. Protein Chem.*, **24**, 309–41.

Bulpin, P.V., Cutler, A.N. & Dea, I.C.M. (1984). Thermally-reversible gels from low DE maltodextrins. In *Gums and Stabilisers for the Food Industry — 2*, ed. G.O. Phillips, D.J. Wedlock & P.A. Williams. Pergamon, Oxford, pp. 475–84.

Busnel, J.P., Clegg, S.M. & Morris, E.R. (1988). Melting behaviour of gelatin gels: origin and control. In *Gums and Stabilisers for the Food Industry — 4*, ed. G.O. Phillips, D.J. Wedlock & P.A. Williams. IRL Press, Oxford, pp. 105–15.

Clark, A.H., Gidley, M.J., Richardson, R.K. & Ross-Murphy, S.B. (1989). *Macromolecules*, **22**, 346–51.

Djerasi, C. (1960). *Optical Rotatory Dispersion: Applications to Organic Chemistry*. McGraw-Hill, New York.

Flory, P.J. & Rehner, J. Jr. (1943). *J. Chem. Phys.*, **11**, 512–20.

Gidley, M.J. (1985). *Carbohydr. Res.*, **139**, 85–93.

Gidley, M.J. (1989). *Macromolecules*, **22**, 351–8.

Gidley, M.J. & Bulpin, P.V. (1987). *Carbohydr. Res.*, **161**, 291–300.

Gidley, M.J. & Bulpin, P.V. (1989). *Macromolecules*, **22**, 341–6.

Husemann, E., Pfannemüller, B. & Burchard, W. (1963). *Makromol. Chem.*, **59**, 1–15.

Husemann, E., Burchard, W. & Pfannemüller, B. (1964). *Stärke*, **16**, 143–50.

Jane, J.-L. & Robyt, J.F. (1984). *Carbohydr. Res.*, **132**, 105–18.

Kasapis, S., Morris, E.R., Norton, I.T. & Clark, A.H. (1993*a*). *Carbohydr. Polym.*, **21**, 243–8, this issue. (Part I of series.)

Kasapis, S., Morris, E.R., Norton, I.T. & Brown, C.R.T. (1993*b*). *Carbohydr. Polym.*, **21**, 261–8, this issue. (Part III of series.)

Koningsveld, R. (1968). *Adv. Colloid Interface Sci.*, **2**, 151–215.

Morawetz, H. (1965). *Macromolecules in Solution*. Wiley, New York.

Pfannemüller, B. (1987). *Int. J. Biol. Macromol.*, **9**, 105–8.

Pfannemüller, B., Mayerhöfer, H. & Schulz, R.C. (1971). *Biopolymers*, **10**, 243–61.

Richter, M., Schierbaum, F., Augustat, S. & Knoch, K.-D. (1976). US Patent no. 3 962 465.

Ring, S.G., Colonna, P., I'Anson, K.J., Kalichevsky, M.T., Miles, M.J., Morris, V.J. & Orford, P.D. (1987). *Carbohydr. Res.*, **162**, 277–93.

Schierbaum, F., Richter, M., Augustat, S. & Radosta, S. (1979). *Dtsch. Lebensmittel-Rdsch.*, **73**, 390–4.

Schierbaum, F., Vorwerg, W., Kettlitz, B. & Reuther, F. (1986). *Nahrung*, **30**, 1047–9.

Tolstoguzov, V.B. (1986). Functional properties of protein–polysaccharide mixtures. In *Functional Properties of Food Macromolecules*, ed. J.R. Mitchell & D.A. Ledward. Elsevier, London, pp. 385–415.

Tolstoguzov, V.B. (1988). *Food Hydrocolloids*, **2**, 339–70.

Tolstoguzov, V.B. (1991). *Food Hydrocolloids*, **4**, 429–68.

Tolstoguzov, V.B. & Wajnermann, E.S. (1975). *Nahrung*, **19**, 45–60.

Whistler, R.L. & Paschall, E.F. (1967). *Starch: Chemistry and Technology*. Academic Press, New York.

Zhuravskaya, N.A., Kiknadze, E.V., Antonov, Yu. A. & Tolstoguzov, V.B. (1986). *Nahrung*, **30**, 591–9.